



## On nonlinear diffusion with multiplicative noise

To cite this article: M. A. Muñoz and T. Hwa 1998 *EPL* **41** 147

View the [article online](#) for updates and enhancements.

### You may also like

- [Characteristics of Cantilever Retaining Wall Composed of Upper Wall and Lower Wall by Physical Testing](#)  
Yaming Zhang, Dongsheng Chen, Jinlong Liu et al.
- [On the emergence of traffic jams in a stochastic traffic flow driven by additive and multiplicative white Gaussian noise processes](#)  
Aman Kumar Singh, Jarrett Meyer and Subramanian Ramakrishnan
- [Multiplicative noise in Euclidean Schwarzschild manifold](#)  
M S Soares, N F Svaiter and C A D Zarro

## On nonlinear diffusion with multiplicative noise

M. A. MUÑOZ<sup>1,2</sup> and T. HWA<sup>1</sup>

<sup>1</sup> *Department of Physics, University of California at San Diego  
La Jolla, CA 92093-0319, USA*

<sup>2</sup> *Dipartimento di Fisica, Università di Roma "La Sapienza"  
P.le A. Moro 2, I-00185 Roma, Italy*

(received 4 August 1997; accepted 27 November 1997)

PACS. 47.20Ky – Nonlinearity (including bifurcation theory).

PACS. 74.40+k – Fluctuations (noise, chaos, nonequilibrium superconductivity, localization, etc.).

**Abstract.** – Nonlinear diffusion is studied in the presence of multiplicative noise. The nonlinearity can be viewed as a “wall” limiting the motion of the diffusing field. A dynamic phase transition occurs when the system “unbinds” from the wall. Two different universality classes, corresponding to the cases of an “upper” and a “lower” wall, are identified and their critical properties are characterized. While the lower wall problem can be understood by applying the knowledge of *linear* diffusion with multiplicative noise, the upper wall problem exhibits an anomaly due to an effective long-ranged repulsion exerted by the wall.

The diffusion equation with multiplicative noise has been used as a paradigm to describe a large class of nonequilibrium dynamical processes [1]. These include the propagation of light in random media [2], the growth of bacterial colonies in changing nutrient environments [3], and the fluctuation of wealth in economic systems [4]. In this paper, we study the effect of nonlinearities, which inevitably occur in such processes due to the existence of characteristic scales of the diffusing fields. For instance, the growth of a population is bounded from above by a characteristic density determined by the competition of resources [5], and an investor’s wealth can be taken as bounded from below by a fixed income source [6], [7]. At sufficiently coarse-grained scales, these effects may be captured by the following *nonlinear* diffusion equation with multiplicative noise:

$$\partial_t n = \nabla^2 n + a n - b n^{1+p} + n(\mathbf{x}, t) \eta(\mathbf{x}, t), \quad (1)$$

where  $a$  and  $b$  are constants,  $p$  specifies the degree of nonlinearity, and  $\eta(\mathbf{x}, t)$  is a Gaussian noise with zero mean and the variance  $\langle \eta(\mathbf{x}, t) \eta(\mathbf{x}', t') \rangle = 2D \delta(\mathbf{x} - \mathbf{x}') \delta(t - t')$ . (Note that eq. (1) should be interpreted either in the Ito or Stratonovich sense [8], depending on the details of the specific process being considered.) We shall fix the coefficient  $b$  to be  $p$  from here on, so that for  $p > 0$  the nonlinear term acts like a soft *upper wall* preventing  $n(\mathbf{x}, t)$  from reaching large values even if  $a$  is large and positive, while for  $p < 0$  the nonlinear term acts like a soft *lower wall* repelling  $n(\mathbf{x}, t)$  from approaching zero even for large and negative  $a$ ’s. The specific choice of  $p$  depends on the symmetries and constraints of the system: For instance,  $p = 1$  is the natural choice for the bacteria growth problem,  $p = 2$  is needed to describe nonlinear effects in quantum optics, while  $p = -1$  is appropriate for modeling a steady income source for the investor in an economic system. The limits  $p \rightarrow \pm\infty$  mimic the effect of *hard* upper/lower walls and are also of interest.

By making use of the Cole-Hopf transform,  $h(\mathbf{x}, t) = \log n(\mathbf{x}, t)$ , we get

$$\partial_t h = \nabla^2 h + (\nabla h)^2 + (a - a_0) - p e^{\text{ph}} + \eta(\mathbf{x}, t), \quad (2)$$

which is a Langevin equation similar to the KPZ equation describing the kinetic roughening of a growing interface  $h$  [9], [10], with an additional drift term  $a - a_0$  ( $a_0 = 0$  for Stratonovich dynamics and  $a_0 = D$  for Ito dynamics [8]), and an “exponential wall” at  $h \approx 0$ . Thus a wall in the diffusion problem corresponds to a wall also in the interface problem. Equation (2) shows that the sign of  $p$  determines the *orientation* of the wall while the magnitude of  $p$  describes the hardness of the wall. In the interface representation, it is clear that for large positive (negative)  $a$ ’s, the system is pushed against the upper (lower) wall, while for large negative (positive)  $a$ ’s, the system is pushed away from the wall to  $h = -\infty$  ( $h = +\infty$ ), corresponding to  $n = 0$  ( $n = \infty$ ). A critical point separates the two regimes where the system “unbinds” from the wall. In this paper, we study the nature of this *dynamic unbinding transition* for walls characterized by different  $p$ ’s. We will show that while the soft and hard walls yield the same critical phenomena, the upper and lower walls yield two *different* universality classes.

We start with a review of the exactly solvable zero-dimensional problem [11]. Without spatial couplings in eq. (2), the stationary distribution is simply

$$\tilde{P}(h) \propto \exp \left[ \frac{a - a_0}{D} h \right] \cdot \exp \left[ -\frac{1}{D} e^{\text{ph}} \right], \quad (3)$$

where the second exponential merely enforces the constraint of the wall, *i.e.* it suppresses  $\tilde{P}$  for  $h > 0$  ( $h < 0$ ) if  $p > 0$  ( $p < 0$ ). From (3), the stationary distribution of  $n$  is easily obtained using the relation  $P(n) = n^{-1} \tilde{P}(\log n)$ , yielding  $P(n) \propto n^{[(a-a_0)/D]-1} \exp[-n^p/D]$ . Note that the distribution functions are normalizable as long as  $(a - a_0) \cdot p > 0$ . Hence a power law distribution in  $n$  is obtained for a large range of parameter values. (A similar result was obtained previously for the case of a hard lower wall [6], [7].)

As  $a \rightarrow a_0^\pm$ , the average  $h$  diverges according to eq. (3) as  $\langle h \rangle \sim \mp |a - a_0|^{-1}$  for the upper/lower wall, indicating the onset of an “unbinding transition” of  $h$  from the wall. This transition can be characterized quantitatively by singularities in moments of  $n$ . From  $P(n)$ , we find for the upper wall problem  $\langle n^m \rangle \sim (a - a_0)^{\beta_m}$  and  $\beta_m = 1$  for all integer  $m$ ’s. The distribution collapses towards  $P(n) = \delta(n)$  as  $a \rightarrow a_0^+$ . For the lower wall,  $\langle n^m \rangle$  diverge as  $a \rightarrow a_0^-$  since  $P(n)$  has no upper cut-off. It is convenient to characterize the phase transition in this case by monitoring  $\bar{n} \equiv 1/n$ . One finds  $\langle \bar{n}^m \rangle \sim (a_0 - a)^{\bar{\beta}_m}$ , with  $\bar{\beta}_m = 1$  also. The symmetry between the upper and lower wall problems is evident from the  $h \rightarrow -h$  symmetry of eq. (2) in the absence of spatial couplings. Note that the asymptotic critical properties given above are independent of the parameter  $p$ , indicating that in the vicinity of the unbinding transition, where  $\langle n \rangle$  approaches zero or infinity (or as  $\langle h \rangle \rightarrow \mp\infty$ ), the detailed form of the wall at finite  $n$  (or at  $h \approx 0$ ) is *irrelevant*.

Time-dependent properties of the system can be obtained by solving the full Fokker-Planck equation [8], [11]. Qualitative features can be obtained alternatively by considering the simpler Langevin equation for  $h(t)$ . We illustrate the solution by analyzing the problem with a lower wall ( $p < 0$ ). For  $a < a_0$ ,  $h$  is confined to the range  $0 < h < \delta h$ , where  $\delta h \sim (a_0 - a)^{-1}$  is the scale of typical fluctuations in  $h$ . Right at the critical point  $a = a_0$ ,  $\delta h$  diverges, *i.e.*  $\delta h(t) \rightarrow \infty$  as  $t \rightarrow \infty$ . The form of  $\delta h(t)$  is dictated by the equation of motion at the critical point,  $\partial_t h = -p e^{\text{ph}} + \eta(t)$ .  $\delta h(t)$  must be *at least* of  $O(t^{1/2})$  due to the random forcing  $\eta$ ; the presence of the wall can only speed up the motion away from the wall. On the other hand, as  $h$  drifts far away from the wall, it should not be affected by the wall. Thus  $\delta h(t) \sim t^{1/2}$  at the transition, with the distribution given by the scaling form  $\tilde{P}(h, t) = (\delta h)^{-1} g[h/\delta h(t)]$ , for

$p \cdot h < 0$ . Here the factor  $(\delta h(t))^{-1}$  provides the proper normalization, and  $g(y)$  is a scaling function with the limiting behaviors  $g(y) \approx \text{const}$  for  $|y| \ll 1$  and  $g(y) \rightarrow 0$  for  $|y| \gg 1$ . Now, it is trivial to derive  $P(n, t)$ , and from it  $\langle n^m \rangle \sim \delta h \sim t^{1/2}$  for all positive moments  $m$ .

We now proceed to characterize the behavior of the system in arbitrary spatial dimension  $d$ . This is accomplished by generalizing the above zero-dimensional picture and utilizing the known properties of the KPZ equation in finite dimensions [9], [10]. The Cole-Hopf transformation has already been exploited in ref. [12] to derive some properties of the system with a soft upper wall ( $p > 0$ ). Some of the arguments there (but not all [13]) can be generalized also to the case of a lower wall.

Close to the critical point,  $h(\mathbf{x}, t)$  is on average far from the wall, and the main source of fluctuation comes from the stochastic KPZ equation without walls, for all length scales below the correlation length  $\xi$ . The scaling properties of the KPZ equation can be described in terms of the dynamic exponent  $z$  alone [9]: the typical correlation time is  $\tau \sim \xi^z$  and typical height fluctuation is  $\delta h \sim \xi^{2-z}$ . These properties yield the scaling form for the additive renormalization  $\langle (\nabla h)^2 \rangle$  of the bare drift  $(a - a_0)$ , with  $\langle (\nabla h)^2 \rangle = a_1 - a_2(\xi)$ , where  $a_1 \propto D$  is a constant and  $a_2(\xi) \sim (\delta h/\xi)^2 \sim \xi^{-1/(2z-2)}$ . Thus one finds  $\xi \sim |a - a_c|^{-\nu}$  with  $a_c = a_0 - a_1$  and  $\nu = 1/(2z - 2)$  for both the upper and lower wall. In particular, in one dimension where it is known exactly that  $z = 3/2$ , we have  $\nu = 1$ . The exponents  $\nu$  and  $z$  can be used to relate the exponents  $\beta$  ( $\bar{\beta}$ ) and  $\theta$  ( $\bar{\theta}$ ) which describe the behavior of the “order parameter”  $n$  ( $\bar{n} = n^{-1}$ ) close to the critical point for the problem with an upper (lower) wall. From the definitions  $\langle n^m \rangle \sim |a - a_c|^{\beta_m}$  and  $\langle n^m \rangle \sim t^{-\theta_m}$  at  $a = a_c$ , it follows that  $\theta_m = \beta_m/(\nu z)$ ; similarly,  $\bar{\theta}_m = \bar{\beta}_m/(\nu z)$ .

To find the exponents  $\beta$  and  $\theta$ , we first perform a naive scaling analysis. Let us assume that at the critical point,  $\hat{P}(h, t)$  is still given by the scaling form of the 0d case, but with  $\delta h(\tau) \sim \tau^\omega$ , where  $\omega = (2 - z)/z$  in  $d > 0$ . (We will return shortly to examine the validity and significance of this assumption.) It then follows that  $\langle n^m \rangle_{\text{upper}} \sim \langle \bar{n}^m \rangle_{\text{lower}} \sim \delta h$  as before, yielding  $\theta_m = \bar{\theta}_m = \omega = (2 - z)/z$  and  $\beta_m = \bar{\beta}_m = (2 - z)/(2z - 2)$  for all  $m$ 's. These exponents take on the value  $\theta = 1/3$ ,  $\beta = 1/2$  in 1d and  $\theta \approx 0.25$  and  $\beta \approx 0.33$  in 2d.

So far we have not distinguished between systems with a lower or upper wall. On the other hand, it is evident that the equation of motion (2) for  $p > 0$  and  $p < 0$  are different in finite  $d$  due to the presence of the nonlinear term  $(\nabla h)^2$ . Thus the problems with upper and lower wall can no longer be mapped onto each other. In order to see whether the orientation of the wall is relevant to criticality, and whether the above scaling ansatz is correct, we perform a numerical simulation in one spatial dimension.

We consider a discrete model which, in the absence of walls, belongs to the KPZ universality class [10]. At each point  $x$  of a one-dimensional lattice of size  $L$ , we define a continuous height variable,  $h_t(x)$ . At each time step a new variable  $h'(x) = h_t(x) + a + \eta_t(x)$  is obtained, with  $\eta_t(x)$  being a random number uniformly distributed in  $[0, 1]$ . The lattice is updated simultaneously according to the rule  $h_{t+1}(x) = \max[h'(x \pm 1) + \gamma, h'(x, t)]$ , and periodic boundary condition is applied. Different values of  $\gamma$  yield qualitatively the same behavior. For the results reported below, we take those obtained with  $\gamma = 0.1$ . The parameter  $a$  controls the drift of the system and is the only tuning parameter. A *hard wall* at  $h = 0$  is introduced by including the additional rule  $h_t(x) = \min[h_t(x), 0]$  for an upper wall or  $h_t(x) = \max[h_t(x), 0]$  for a lower wall. The algorithm for lower wall is almost identical to the one used in local alignment of DNA sequences [14].

We describe first the results for an upper wall. The first step to studying critical properties is to locate the critical point accurately. Starting with the initial condition,  $h_0(x) = 0$  for all  $x$ , we let the system evolve long enough so that a stationary state is reached and we average over up to 1000 independent runs. For a given size  $L$ , the critical point  $a_c(L)$  is taken as the first

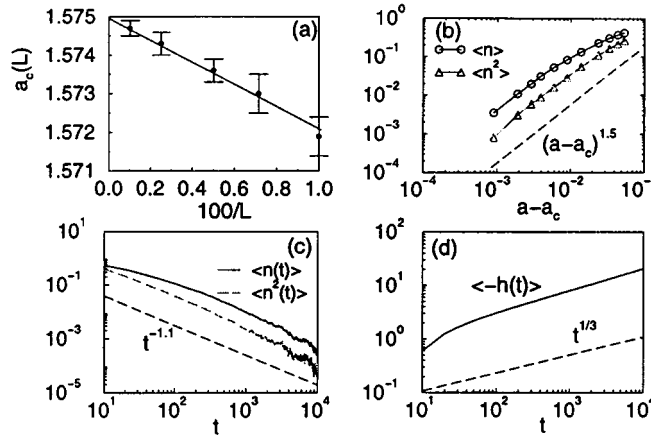


Fig. 1. – Results with an upper wall: (a) Size dependence of the critical point  $a_c(L)$ ; (b) first two moments of the spatially averaged  $n$  vs.  $a - a_c$  in the steady state; (c) time dependence of  $\langle n \rangle$  and  $\langle n^2 \rangle$  at  $a = a_c$ ; (d)  $\langle -h(t) \rangle$  at  $a = a_c$ .

value of  $a$  for which the steady-state value  $\langle n \rangle = \langle \exp(h) \rangle$  becomes indistinguishable from zero as  $a$  is decreased. A plot of  $a_c(L)$  vs.  $1/L$  is shown in fig. 1 (a). Linearity of the data suggests  $\nu \approx 1$ . Extrapolating to  $L \rightarrow \infty$ , we get  $a_c \approx -1.5750$ . The scaling of  $\langle n \rangle$  and  $\langle n^2 \rangle$  upon approaching the critical point  $a_c(L)$  is shown in fig. 1 (b) for  $L = 400$ . We obtain the exponents  $\beta_1 \approx \beta_2 = 1.50 \pm 0.15$ . In fig. 1 (c), we plot  $\langle n(t) \rangle$  and  $\langle n^2(t) \rangle$  vs.  $t$  at  $a = a_c$ , and find  $\theta_1 \approx \theta_2 = 1.10 \pm 0.12$ . The scaling of  $\langle h \rangle$  at  $a = a_c$  is shown in fig. 1 (d). We find the exponent  $\omega \approx 0.33$ . To compute the dynamic exponent  $z$ , we perform a slightly different simulation [15]: We take as initial condition a state in which  $h$  is a large negative constant at every lattice point except for the origin where  $h_0 = 0$ . The spreading of this “seed” is followed, and from the time evolution of the average size of the “infected region”, we find  $z = 1.50 \pm 0.05$ . All the measured exponents coincide, within numerical accuracy, with those computed previously [12] for eq. (1) with  $p = 1, 2$ , i.e. soft walls. This indicates that the introduction of an upper soft or a hard wall to a model belonging to the KPZ universality class yields the same critical behavior. As found in ref. [12], the exponents  $\nu$  and  $z$  agree with the result of the scaling analysis. Also the scaling relation  $\theta_m = \beta_m/(\nu z)$  [12], [15] is satisfied. However, the values of  $\beta$  and  $\theta$  are significantly different from those derived above using the naive scaling analysis.

We next describe the results for a lower wall. Following the same analysis for  $\langle \bar{n} \rangle$ , we obtain  $a_c \approx -1.5743$ , and  $\nu \approx 1$  (fig. 2 (a)). From fig. 2 (b), we find  $\bar{\beta}_1 \approx \bar{\beta}_2 = 0.48 \pm 0.05$  [13] and from figs. 2 (c) and (d), we find  $\bar{\theta}_1 \approx \bar{\theta}_2 = 0.32 \pm 0.03$ ,  $\omega = 0.33 \pm 0.04$ . The dynamic exponent  $z \approx 1.5$  is determined using the seed-spreading method. Note that in contrast to the upper-wall problem, all the exponents here are consistent with the expected results based on the naive scaling analysis, including the values of  $\bar{\beta}$  and  $\bar{\theta}$ . The clear difference between  $\beta, \theta$  and  $\bar{\beta}, \bar{\theta}$  indicate that *problems with upper and lower walls belong to different universality classes*.

As the fluctuations in  $\langle h(t) \rangle$  obey the same scaling law ( $\omega \approx 0.33$ ) for both the upper and lower wall problems (figs. 1 (d) and 2 (d)), differences in the scaling of  $\langle n^m \rangle_{\text{upper}}$  and  $\langle \bar{n}^m \rangle_{\text{lower}}$  must result from differences in the distribution  $\tilde{P}(h, t)$ , or more specifically, in the form of the scaling functions  $g(h/t^\omega)$ . The numerics suggests that the 0-d behavior of  $g(y) \approx \text{const}$  for  $|y| < 1$  and  $g(y) \rightarrow 0$  for  $y \gg 1$  is obtained in 1d for the lower wall problem only. The numerically obtained forms of the scaling function  $g(h/t^{1/3})$  for the upper and lower wall are presented in fig. 3 (a) and (b), respectively. Note that for large  $|h|/t^{1/3}$ , the

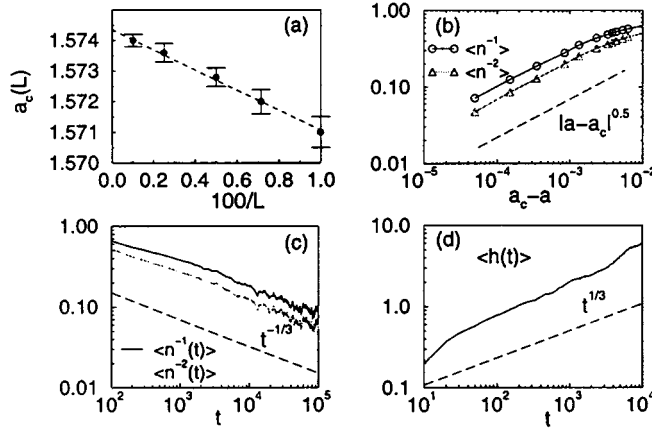


Fig. 2. – Results with a lower wall: (a) Size dependence of the critical point  $a_c(L)$ ; (b) first two moments of the spatially averaged  $\bar{n}$  vs.  $a_c - a$  in the steady state; (c) time dependence of  $\langle \bar{n} \rangle$  and  $\langle \bar{n}^2 \rangle$  at  $a = a_c$ ; (d)  $\langle h(t) \rangle$  at  $a = a_c$ .

distribution function drops off sharply (approximately exponentially) in both cases. Thus the assumed form for the scaling function  $g(y)$  is satisfied for large  $y$ . However, the distributions are qualitatively different for small values of  $|h|/t^{1/3}$ , reflecting qualitative differences in the interaction between  $h$  and the upper/lower wall at  $h = 0$ . To appreciate the origin of this difference, let us consider the evolution of a piece of *flat* interface  $h = 0$  at the critical point  $a = a_c = a_0 - a_1$ . The local drift rate  $\langle \partial_t h \rangle \approx \langle (\nabla h)^2 \rangle - a_1$  is *negative* since  $h = 0$  and  $\nabla h = 0$  there. In the case of a lower wall, this negative drift has no effect since the interface cannot penetrate below the wall. A steady state results from a dynamic balance between the driving force ( $a - a_c < 0$ ) which “flattens” pieces of the interface against the wall, and the noise  $\eta$  which roughens the interface. Thus, the situation is very similar to the zero-dimensional case, and we expect the exponent results obtained above from the naive scaling analysis to be valid for all  $d$ . The situation is very different for the case of an upper wall, since the negative drift represents a significant force *repelling* the interface from the wall. The effective repulsion exerted by the upper wall is in fact *long ranged*: Suppose the interface is on average at a distance  $\bar{h}$  from the wall. Then interfacial roughness is “interrupted” by the wall at a scale  $\bar{\xi} \sim \bar{h}^2$  in 1d, leading

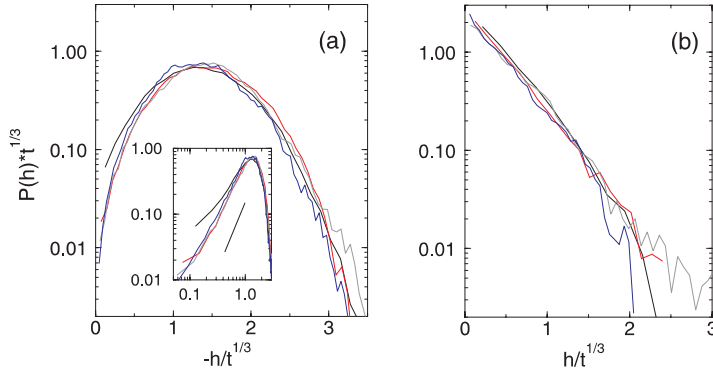


Fig. 3. – Scaled probability distribution  $\tilde{P}(h, t) \cdot t^{1/3}$  for 10 samples of size  $L = 3000$ , with (a) an upper wall (inset: log-log plot; straight line indicates  $(|h|/t^{1/3})^2$ ), and (b) a lower wall. The different curves are for  $t = 500, 2500, 5000, 10000$ .

to an effective repulsive force  $\langle \partial_t h \rangle \sim -1/\bar{\xi}^\nu \sim -1/\bar{h}^2$ . Thus, a steady state can only be achieved by keeping the interface *away* from the wall. This necessarily leads to the *depletion* of  $\tilde{P}(h, t)$  for small  $|h|$ . We expect  $\tilde{P}$  to have a power law form,  $\tilde{P}(h, t) \sim (|h|/t^{1/3})^\sigma$  for  $|h| \ll t^{1/3}$ . Our numerical results (fig. 3 (a) inset) are consistent with such a form, with  $\sigma \approx 2$ . The new form of  $\tilde{P}$  for the upper wall allows us to obtain moments of  $n$  in terms of  $\sigma$ . We find  $\theta_m = (1 + \sigma) \cdot \omega \approx 1$ . Our numerical result  $\theta_m \approx 1.1 \pm 0.1$  (fig. 1 (c)) is consistent with this relation.

Away from the critical point, the form of  $\tilde{P}(h)$  is simply obtained by replacing  $\delta h(t) \sim t^\omega$  with  $|a - a_c|^{-\nu(2-z)} = |a - a_c|^{-1/2}$  in  $d = 1$ . Our numerics for the lower wall problem (fig. 3 (b)) suggests that  $\tilde{P}(h) \propto \exp[-ch(a_c - a)^{1/2}]$ , where  $c$  is a nonuniversal constant. This exponential distribution of  $h$  (confirmed by numerics) leads to a power law form for  $P(n)$  as in the 0d case. Again, we expect this result to hold in all  $d$ . For the upper-wall problem, the depletion effect described by the extra factor  $[|h|(a - a_c)^{1/2}]^\sigma$  in  $\tilde{P}(h)$  leads to logarithmic corrections to the power law form of  $P(n)$ .

In summary, nonlinear diffusion with multiplicative noise has been analyzed in terms of a *dynamic unbinding transition* from a wall. Two distinct universality classes are obtained for the upper and lower walls in finite spatial dimensions. A detailed physical picture is constructed to elucidate the mechanism leading to the differences: The upper-wall problem exhibits anomalous scaling due to a long-ranged effective repulsion exerted by the wall. A new exponent relation, linking the anomalous critical exponents to singularity in the probability distribution function, is proposed and verified numerically. The repulsion is absent in the lower-wall problem, and the scaling behaviors there can be understood completely by combining and applying the knowledge of the 0d problem and the KPZ equation.

\*\*\*

We are grateful to M. LÄSSIG, YUHAU TU, G. GRINSTEIN and A. V. GRUZINOV for discussions. MAM acknowledges the hospitality at UC San Diego. TH is supported by an A. P. Sloan Research Fellowship and an ONR Young Investigator Award.

## REFERENCES

- [1] See, e.g., DEUTSCH J. M., *Physica A*, **208** (1994) 445.
- [2] FOCK V. A., *Bull. Acad. Sci. URSS Ser. Phys.*, **14** (1950) 70.
- [3] ZHANG Y.-C., *Phys. Rev. Lett.*, **56** (1986) 2113.
- [4] LEVY M. and SOLOMON S., *Int. J. Mod. Phys. C*, **7** (1996) 65.
- [5] FISHER R. A., *Ann. Eugenics*, **7** (1937) 355.
- [6] LEVY M. and SOLOMON S., *Int. J. Mod. Phys. C*, **7** (1996) 595; 745.
- [7] SORNETTE D. and CONT R., *J. Phys. I*, **7** (1997) 431.
- [8] VAN KAMPEN N. G., *Stochastic Processes in Physics and Chemistry* (North Holland) 1981.
- [9] KARDAR M., PARISI G. and ZHANG Y. C., *Phys. Rev. Lett.*, **56** (1986) 889; MEDINA E. *et al.*, *Phys. Rev. A*, **39** (1989) 3053.
- [10] KRUG J. and SPOHN H., in *Solids far From Equilibrium: Growth, Morphology and Defects*, edited by C. GODRECHE (Cambridge University Press) 1991.
- [11] GRAHAM R. and SCHENZLE A., *Phys. Rev. A*, **25** (1982) 1731; SCHENZLE A. and BRAND H., *Phys. Rev. A*, **20** (1979) 1628.
- [12] TU Y., GRINSTEIN G. and MUÑOZ M. A., *Phys. Rev. Lett.*, **78** (1997) 274; GRINSTEIN G., MUÑOZ M. A. and TU Y., *Phys. Rev. Lett.*, **76** (1996) 4376.
- [13] Note that the calculation used in [12] to derive the bound  $\beta > 1$  for the  $p = 1$  case cannot be extended to  $p < 0$ .
- [14] SMITH T. F. and WATERMAN M. S., *J. Mol. Biol.*, **147** (1981) 195.
- [15] GRASSBERGER P. and DE LA TORRE A., *Ann. Phys. (N.Y.)*, **122** (1979) 373.